

We are IntechOpen, the world's leading publisher of Open Access books Built by scientists, for scientists

6,900

Open access books available

186,000

International authors and editors

200M

Downloads

Our authors are among the

154

Countries delivered to

TOP 1%

most cited scientists

12.2%

Contributors from top 500 universities



WEB OF SCIENCE™

Selection of our books indexed in the Book Citation Index
in Web of Science™ Core Collection (BKCI)

Interested in publishing with us?
Contact book.department@intechopen.com

Numbers displayed above are based on latest data collected.
For more information visit www.intechopen.com



Semisolid Processing of Al/ β -SiC Composites by Mechanical Stirring Casting and High Pressure Die Casting

H. Vladimir Martínez¹ and Marco F. Valencia²

¹*Institute of Energy, Materials and Environment, School of Mechanical Engineering, Pontificia Bolivariana University, Medellín,*

²*Engineering School of Antioquia, Medellín,*

^{1,2}*Colombia*

1. Introduction

Metals and alloys are generally produced and shaped in bulk form but can also be intimately combined with another material that serves to improve their performance. The resulting material is known as a metal matrix composite (MMC). This class of composite encompasses many different materials that can be distinguished according to their base metal (e.g., aluminium, copper, titanium), their reinforcement phase (e.g., fibers, particles, whiskers), or their manufacturing process (e.g., powder metallurgy, diffusion bonding, infiltration, mechanical or electromagnetic stir casting and die casting).

Processing advantages make die casting one of the most efficient technologies available for producing a wide range of durable and rigid MMC products for use in commercial, industrial and consumer applications. There are several well-established die casting methods that can be used to produce castings for specific applications. Including squeeze casting and semisolid molding (thixocasting and rheocasting). Squeeze casting is a method by which molten alloy is cast without turbulence or gas entrapment at high pressure to yield high-quality, dense and heat-treatable components). Thixocasting is a procedure whereby semisolid metal billets, with no dendritic microstructure, are cast to provide dense, heat-treatable castings with low porosity. Rheocasting refers to several processes that allow the creation of globular structures and thixocasting involves the reheating of ingots obtained by rheocasting until the semisolid gap followed by one semisolid molding step.

Modern technology is currently geared towards net-shape processes, which are able to eliminate the intermediate storage of ingots (required in thixocasting), and looking to obtain a more economic process. Despite being known as a pressurization process for melting alloys, die-casting can be used as a post-re-crystallisation, or a semisolid die-casting process. As a result, in this work a high pressure die casting (HPDC) system was integrated with a mechanical stir casting (MSC) system. This MSC&HPDC equipment produces components with near-net shapes in a continuous process that avoids semisolid ingot storage. It is useful

for research and production of MMCs for functional and/or automotive applications. Emphasizing the need for such processes, the current automotive industry regulations for lowering emissions of CO₂ demand a significant vehicle weight reduction. Due to the recent CAFE (CAFE: Corporate Average Fuel Economy) regulations set in North America, the automotive OEMs will have to develop advanced materials and new technologies to meet the new targets set for the industry by 2025. Recent research¹ shows that approximately 50% of the powertrain components of a vehicle will have to be replaced by new parts developed with advanced materials and new technologies.

This chapter traces the development of new materials and processes with a view to improve the quality of aluminum-made parts. Since casting parts have different defectology types, (primarily porosity), net-shape processes provide a way to reduce defects and to increase mechanical properties. Additionally, the main engineering metals and alloys for different components, including aluminum alloys, now have roughly the same $E/\rho \approx 26\text{MJ kg}^{-1}$. Thus the only practical way to exceed this limit in a metallic material is to replace a significant fraction of the metal atoms with a new phase as happens in Al-MMC. In this work the ultimate tensile strength and yield strength at room temperature of Al-Si7-Mg0.3-T6/ β SiC-15wt% composite manufactured by MSC were increased by 73% and 92%, respectively, compared to those of the original alloy with no reinforcement. The elongation of the composite material was decreased 44% because the reinforcement effect.

2. Materials

MMC are mostly aluminium-based alloys reinforced with particles. These alloys include pure aluminium, high-resistance alloys and the very common foundry Al-Si alloys, which allow the synthesis of light composites. In our case it is also important to consider an adequate gap temperature in the semisolid state of the alloy. Thus an Al-Si alloy has been used. Table 1 lists its chemical composition obtained using a Shimadzu spectroscopy 5500-OES.

Si	Fe	Cu	Mg	Mn	Zn	Al
6.5 -7.5	0.2 max	0.2 max	0.25-0.45	0.1 max	0.1 max	balance

Table 1. Chemical composition of the alloy A-356 (wt%).

The mechanical properties of ASTM test specimens made from MMC typically match or approach many of the characteristics of iron castings and steel, at lighter weight. Properties can exceed those of most Al, Mg, Zn or Cu components commonly produced by die casting. Aluminum MMC parts offer higher stiffness and thermal conductivity, improved wear resistance, lower coefficient of thermal expansion, reduced porosity, and higher tensile and fatigue strengths at elevated temperature, with densities within 5% of Al die casting alloys. In addition, particles used as reinforcement are generally less expensive than other reinforcement materials, such as fibers, because of their abundance. Also, some ceramics have far better properties in finely divided form. Notably,

¹ See: <http://www.greencarcongress.com/> (August 2011)

micrometer-sized ceramic fibers or ceramic particles can be much stronger than bulk ceramics. Additionally, small-single-crystal ceramic particles can be excellent conductors of heat. There is a large variety of reinforcing ceramic materials. MMCs commonly are reinforced with silicon carbide (SiC) particles, because of SiC's excellent physical and mechanical properties. SiC can be obtained by several mechanisms, one of which is of particular interest as it contributes greatly to minimizing waste; this procedure involves the controlled pyrolysis of rice husks (RH).

The production method of Martínez & Valencia (2003), designed for the synthesis of SiC from RH, starts with the cleaning, sizing and conditioning the RH before the pyrolysis process. This conditioning is made up of the removal of garbage, size classification by sieving and the use of catalysts to increase the efficiency of the process. $\text{FeCl}_2 \cdot 4\text{H}_2\text{O}$ was used as a catalyst and NH_4OH is used as an agent for precipitation of Fe. Pyrolysis is achieved through controlled thermal decomposition of the RH at 1370°C in an argon atmosphere for 40min. The final product is ground and subjected to a pneumatic separation process and characterization.

Fig. 1 summarizes the analysis of the resulting SiC particles via SEM. Semi-quantitative analysis by EDS yielded the following values: 68.99 wt%C, 23.99 wt%O, 6.42 wt%Si and 0.59 wt%Fe, the latter as a result of the catalyst.

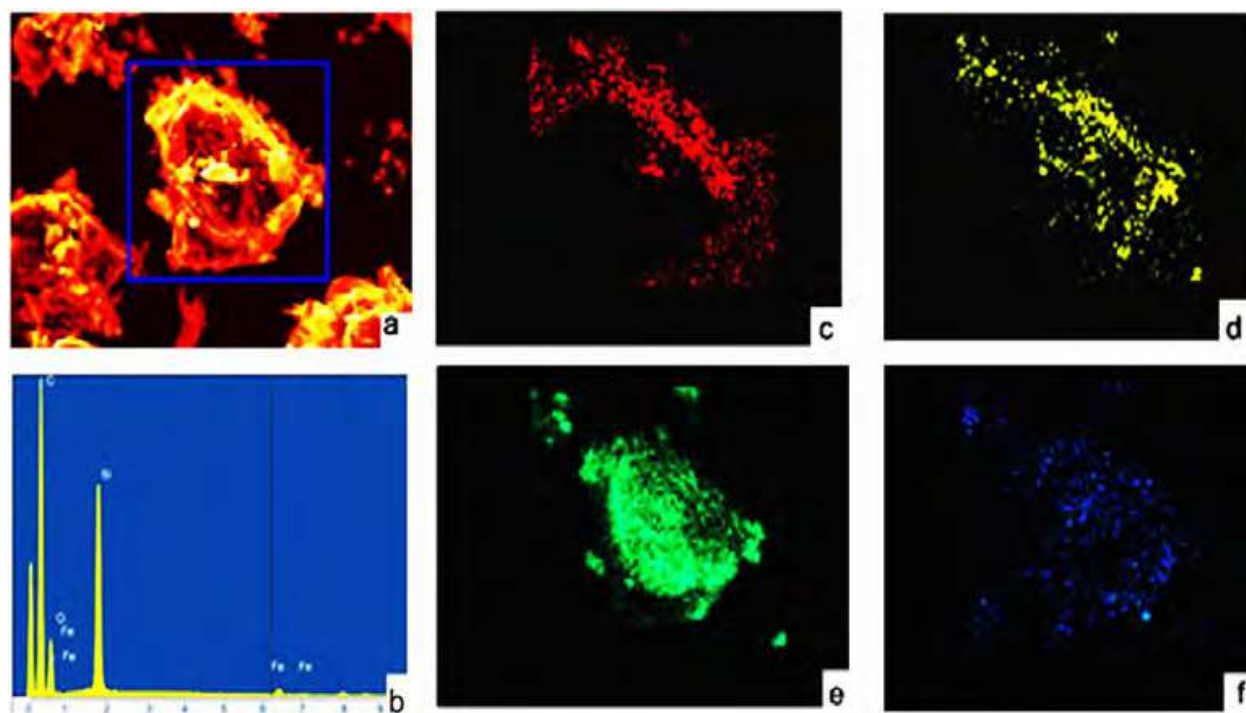


Fig. 1. Elemental mapping of SiC particles obtained by pyrolysis of RH: (a) SEM image, (b) EDS trace (c) C, (d) O, (e) Si, (f) Fe.

The XRD spectrum from the resulting sample has strong peaks at 41.58° and 48.40° , confirming the formation of SiC crystals of the Moissanite (β -SiC) variety (Fig. 2).

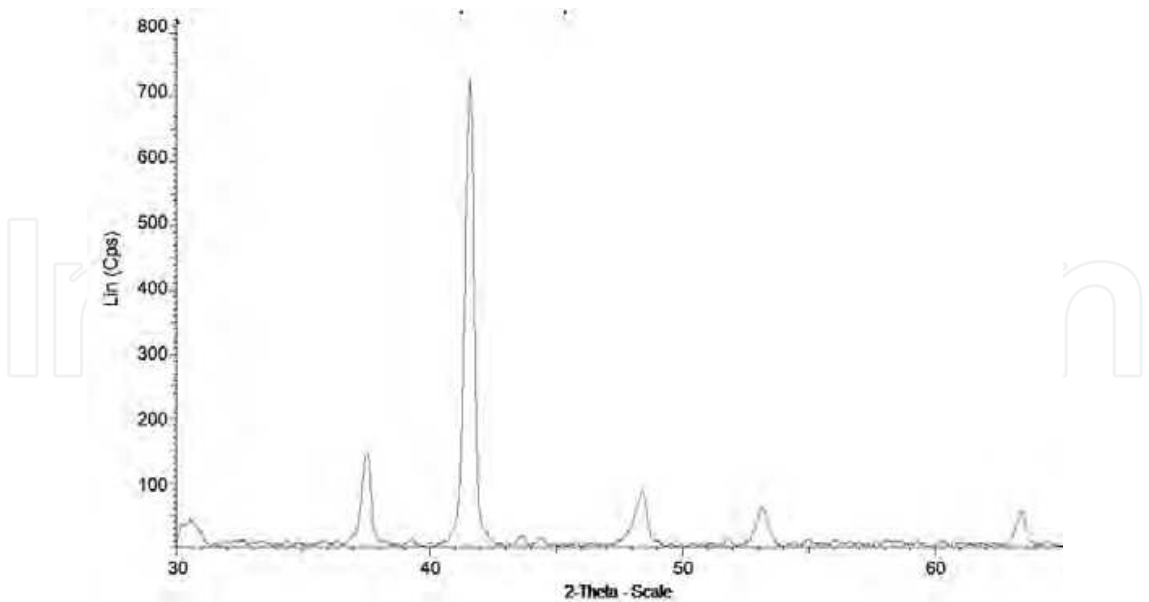


Fig. 2. XRD spectrum of pyrolyzed RH, confirming the formation of SiC.

3. Experimental procedure

In order to synthesize the composite material the difficulties associated with ceramic-metal incompatibility must be resolved; these difficulties are described in terms of the wettability between SiC and aluminum. In addition, avoiding air engulfment during the immersion and dispersion of the reinforcement particles must be ensured. These two requirements and other details of the synthesis process are discussed below.

For semisolid casting, this synthesis process is started with a partially molten aluminum matrix. Once the proper dispersion for the phases has been attained, the conformation process takes place. In this stage the fluid is translated into the cavities of the die casting device, finishing with heat treatments to ensure the required mechanical and physical properties are realized (Fig. 3).

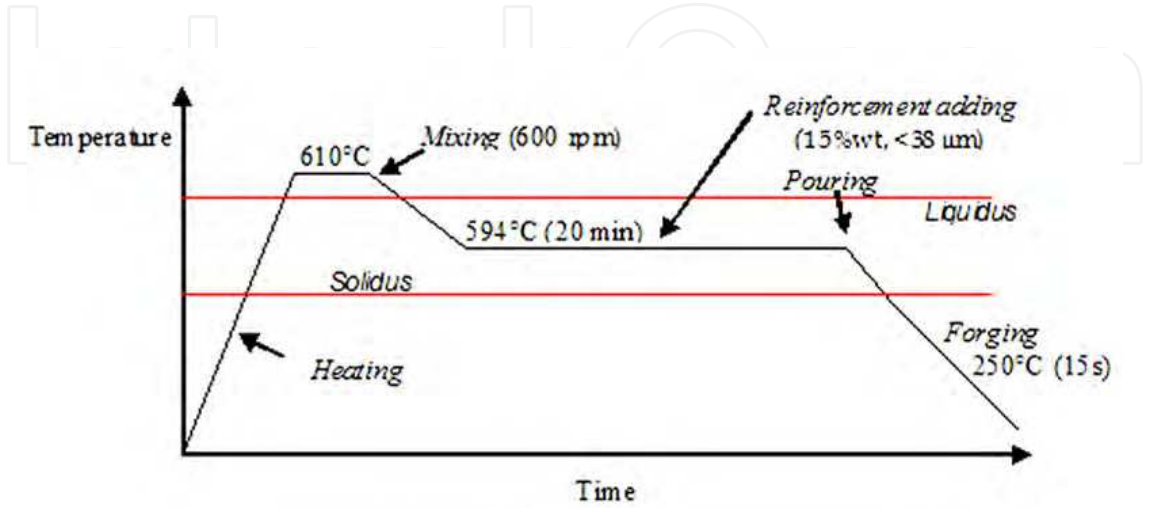


Fig. 3. Production method for Al-MMC.

3.1 Ceramic-metal compatibility

The wettability of SiC by aluminum presents two main difficulties. First, the liquid aluminum reacts with the SiC to form Al_4C_3 near the interface through a dissolution-precipitation mechanism. The formation of Al_4C_3 can be controlled by using low temperatures ($<700^{\circ}C$), which also avoid the sublimation of Mg (vital in the subsequent heat treatment), as well as by minimizing the time between mixing and pouring. In our case, the estimated time was less than 50min. The second difficulty is that the liquid aluminum is normally covered by an oxide layer that inhibits wetting (Laurent, V. et al., 1996). Several possibilities are available to improve wetting between SiC and Al, such as inclusion of reactive elements (e.g. Li, Mg, Si) (Martínez & Valencia, 2004) or using metallic coatings to generate a metal-metal interface, and hence a higher wettability. Previous investigations have shown that the use of Ni or Cu coatings is effective, resulting in an increase in the resistance of the composite, its toughness and a better dispersion of the reinforcement particles within the molten metal (Ghomashchi, 2000). To solve the wetting problems, from the experimental model proposed by Sharma et al. (2006), we proceeded to cover the SiC with Cu deposited by electroless plating (EP); the specific pretreatment, coating and drying, processes are explained in the following section.

3.1.1 Pretreatment

Since the EP technique is a chemical reduction process, the preparation of the surface where the metal will be deposited is essential. That is why the particles were immersed in $SnCl_2$ and $PdCl_2$ solution, respectively. Table 2 lists the details of the pretreatment of the particles.

Solution	Chemical Species	Concentration	Operation	Time (min)
Sensitization	$SnCl_2 \cdot 2H_2O$ HCl	20g/l 0.5 ml/l	Mechanical Stirring (400 rpm)	30
Water wash (pH 7.0) and vacuum filtration				5
Activation (2000 ml)	HCl $PdCl_2$	5.5ml/l 0.25g/l	Mechanical Stirring (400 rpm)	35
Water wash (pH 7.0) and vacuum filtration				5

Table 2. Superficial Pretreatment of β -SiC.

3.1.2 Coating and drying

Once the particles were catalyzed, they were taken to the plating bath, which is constantly stirred, in which the reduction reaction took place (Fig. 4). This bath consists of a metallic ions solution of cupric sulfate, formaldehyde as a reducing agent and sodium-potassium tartrate (Rochelle’s salt) as a complexing agent, which keeps the metallic salt from precipitating. Stirring was maintained and, as the reaction ran out, the solution color changed until it becomes transparent (Fig. 4c), which corresponded to when the Cu from the solution was deposited on the surface of the ceramic particles as metallic Cu.

The temperature of the bath was kept at 80°C while the pH was kept at 12.0. Table 3 summarizes the details of the plating process. As soon as the coating reaction was completed, the particles were washed with water and then dried in a vacuum (~1 bar) at 60°C for one hour.



Fig. 4. Evolution of the plating bath, (a) 0 min, (b) 10 min and (c) 40 min.

Solution	Chemical Species	Value	Role in the bath	Operation	Time (min)
Coating (3000ml)	CuSO ₄ 5H ₂ O	10g/L	Metal ions Coating	Mechanical stirring (1200rpm)	To complete reaction
	CH ₄ O ₆ NaK4H ₂ O	50g/L	Complexing		
	HCHO	15m/L	Reducer		
	NaOH	To adjust pH	Buffer solution for pH control		
Water wash (pH 7.0) and vacuum filtration					5

Table 3. Parameters for the electroless plating of β-SiC.

Fig. 5a is a SEM image of β-SiC particles after the sensitization bath. Fig. 5b shows the qualitative analysis, indicating the presence of Sn, which was used as a catalytic material in the SnCl₂ bath. Fig. 5c shows the coated β-SiC particles. Again, elemental analysis shows the presence of Sn and Pd from the pretreatment process. A high amount of Cu can be observed due to the plating process (Fig. 5d).

By modifying the metal-ceramic interface (SiC-Al) by with a metal-metal type interface (Cu-Al), the micro-composites Cu/β-SiC developed to this point can be introduced into the aluminum to the synthesis of Al-MMC/β-SiC. Kim & Lee (2005) have shown that the sintering of Al-MMC/10wt% SiC, after SiC coating with 8wt%Cu, is significantly improved, achieving a further increase in bending strength. However, the addition of Cu to SiC, with a view to the synthesis of particulate composites Al/β-SiC is limited by the formation of inter-metallic compound CuAl₂ of fragile nature. The formation of this compound is subject to the solubility of Cu in Al, which according to Kim & Lee (2005) is up to 2wt%. This means that

contents at or below 2wt%Cu in Cu/ β -SiC avoid precipitation of Cu and the generation of unwanted inter-metallic compounds. The amount of Cu deposited is a function of coating thickness. In this case it has acted to control the thickness to approximately $<0.6\mu\text{m}$.

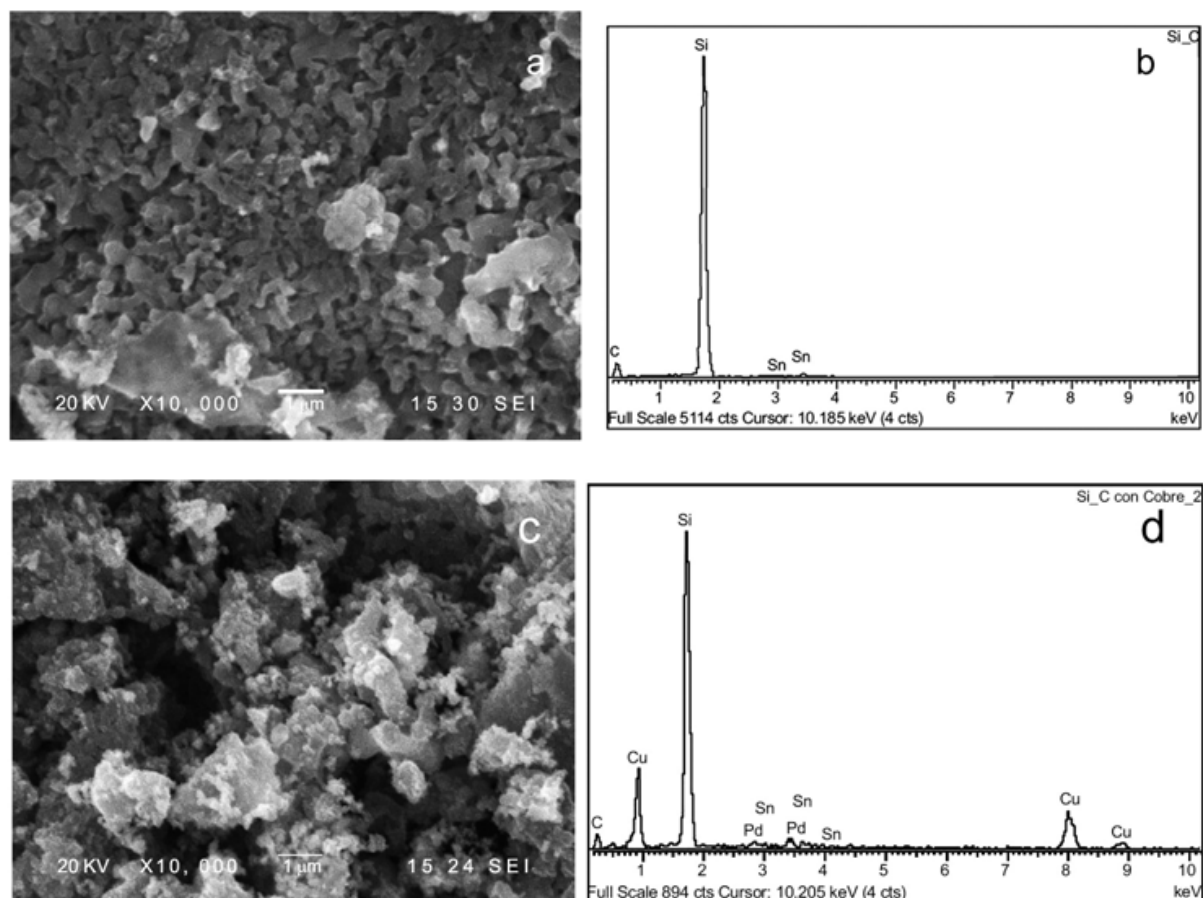


Fig. 5. SEM and EDS for (a), (b) SiC particles without Cu; (c), (d) SiC particles modified with Cu.

3.2 Mechanical Stir Casting (MSC)

In the case of aluminum-silicon alloys, the microstructure is by nature a dendritic type (Yang et al., 2005), which is commonly known as a morphology which decreases the strength of the material depending on the spacing of secondary dendritic arms. During the stirring action it was sought to convert the aluminum microstructure from the semisolid dendritic to a globular form (Mada & Ajersch, 1996). The technique is to generate shear stresses of sufficient magnitude by means of mechanical agitation, causing relative movement between layers and interlaminar friction, that in the best cases, generates a globular morphology (pseudo spheres of about 60 to 72 microns) (Fan, 2002). Nevertheless, a high shear index can be the source of the engulfment of impurities, increasing power consumption and the stress in the rotor system (Biswas et al., 2002). This is why the geometry of the stirring system is a key part in the process. The efficiency, the quasi-isotropy of the material, the micro-structural changes and the transformation the thixotropic

matrix depend on this. Similarly, the agitation system must allow the distribution of reinforcement in the matrix to be uniform, depending on the stirring speed and time in steady state for the molten metal.

With the purpose of increasing the shear efficiency, preventing the formation of an external vortex and obtaining a proper dispersion of the reinforcing material, two trowel systems were studied. In both systems the mechanism was optimized with a set of trowels at 90° - y in the bottom to avoid the sedimentation of non processed material. The two configurations of the upper set of trowels are shown in Fig. 6.

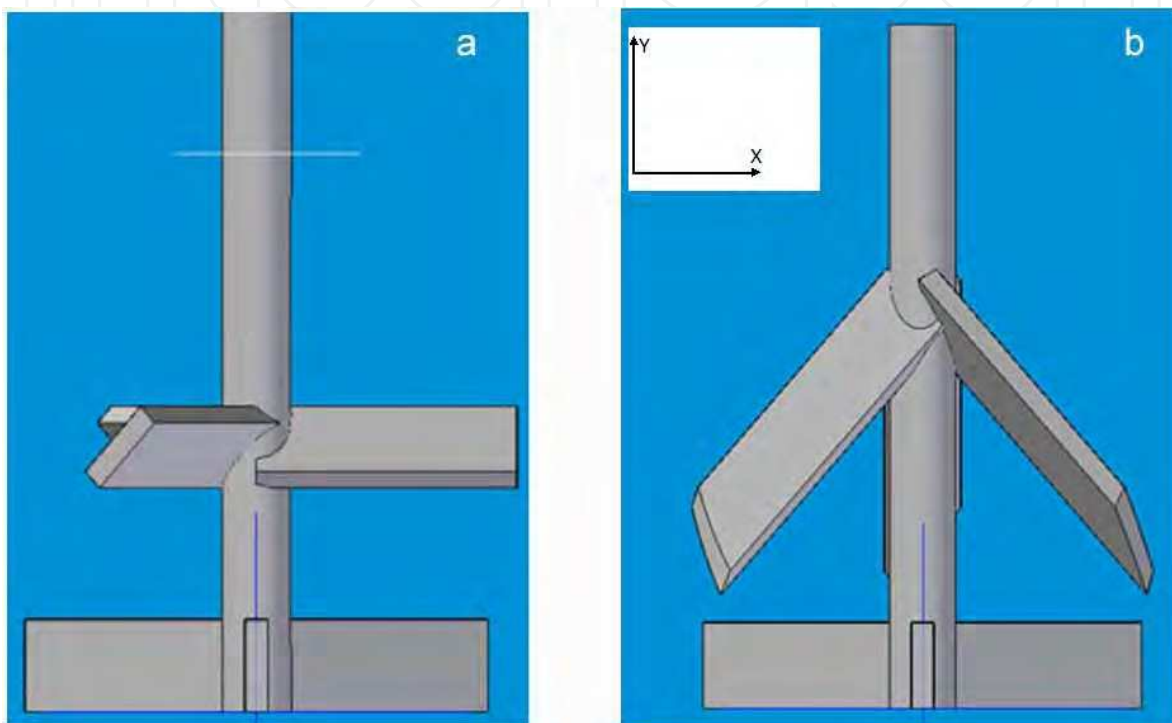


Fig. 6. Two configurations of upper trowels: (a) 45° - x , (b) 45° - $x/45^\circ$ - y .

To ensure adequate mixing conditions the most effective approach is the simulation of the mechanical stir casting (MSC). In this sense, simulations of flow (Flow-3D ®) were initially carried out using computational fluid dynamics (CFD) for each type of agitator to identify the shear rates and changes in material viscosity. The actual process parameters are included in the parameterization of the simulation software (Fig. 3).

3.2.1 Strain rate

The 45° - $x/45^\circ$ - y agitator showed a higher level of shear stress in the fluid, and greater turbulence compared with the 45° - x agitator (Fig. 7a, 7b). For the needs of the mixing process the 45° - $x/45^\circ$ - y stirrer is more efficient as it creates greater strain in the material at the same engine speed. By achieving greater strain on semisolid material a lower viscosity was obtained, ensuring the optimum rheological conditions for the dispersion of the particles.

3.2.2 Viscosity

In both cases it is apparent that the viscosity increases in areas where the agitation generates a low speed level in the fluid, which turns out to be useful to generate tixotropic behavior in the fluid. The 45°-x/45°-y agitator (Fig. 7d) shows a higher viscosity than the 45°-x (Fig. 7c).

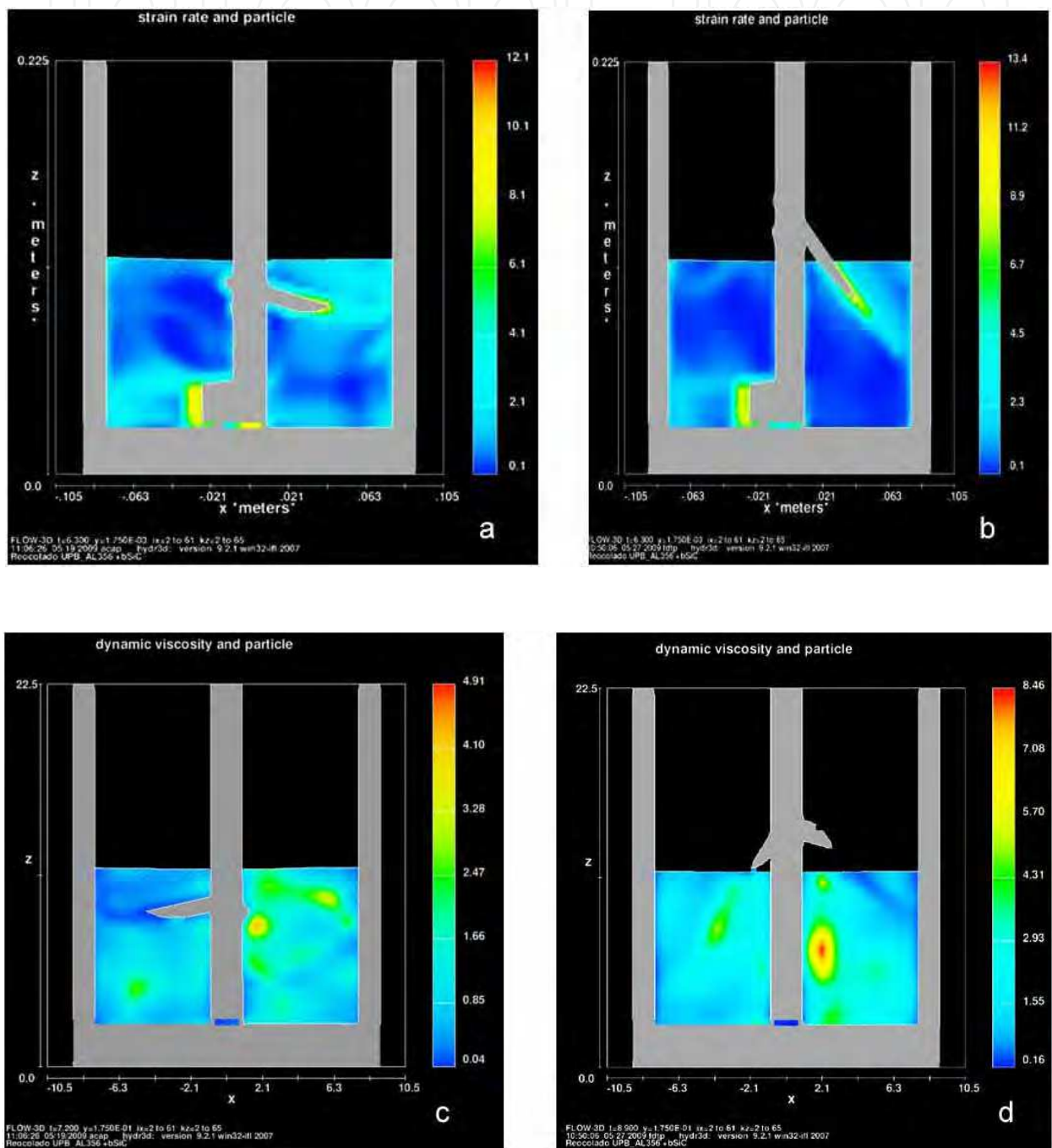


Fig. 7. Simulation of the agitation process. Shear stress profile (a, b) and viscosity (c, d). Agitator 45°-x; (a, c), agitator 45°-x/45°-y (b,d).

3.2.3 Velocity magnitude

The analysis of the agitation a few seconds after the start of the process showed that the fluid velocity reaches a higher value with the agitator $45^\circ\text{-x}/45^\circ\text{-y}$, approximately 26 m/s, while the agitator 45°-x reaches 0.13 m/s (Fig. 8a, 8c).

The dispersion of particles with the $45^\circ\text{-x}/45^\circ\text{-y}$ agitator, when it is not completely immersed, is not as effective as with the 45°-x agitator, and the result is that the particles flow to the bottom of the crucible faster (Fig. 8c). However, the 45°-x and $45^\circ\text{-x}/45^\circ\text{-y}$ configurations allow a homogeneous particle distribution in the radial direction of the crucible (Fig. 8b, 8d).

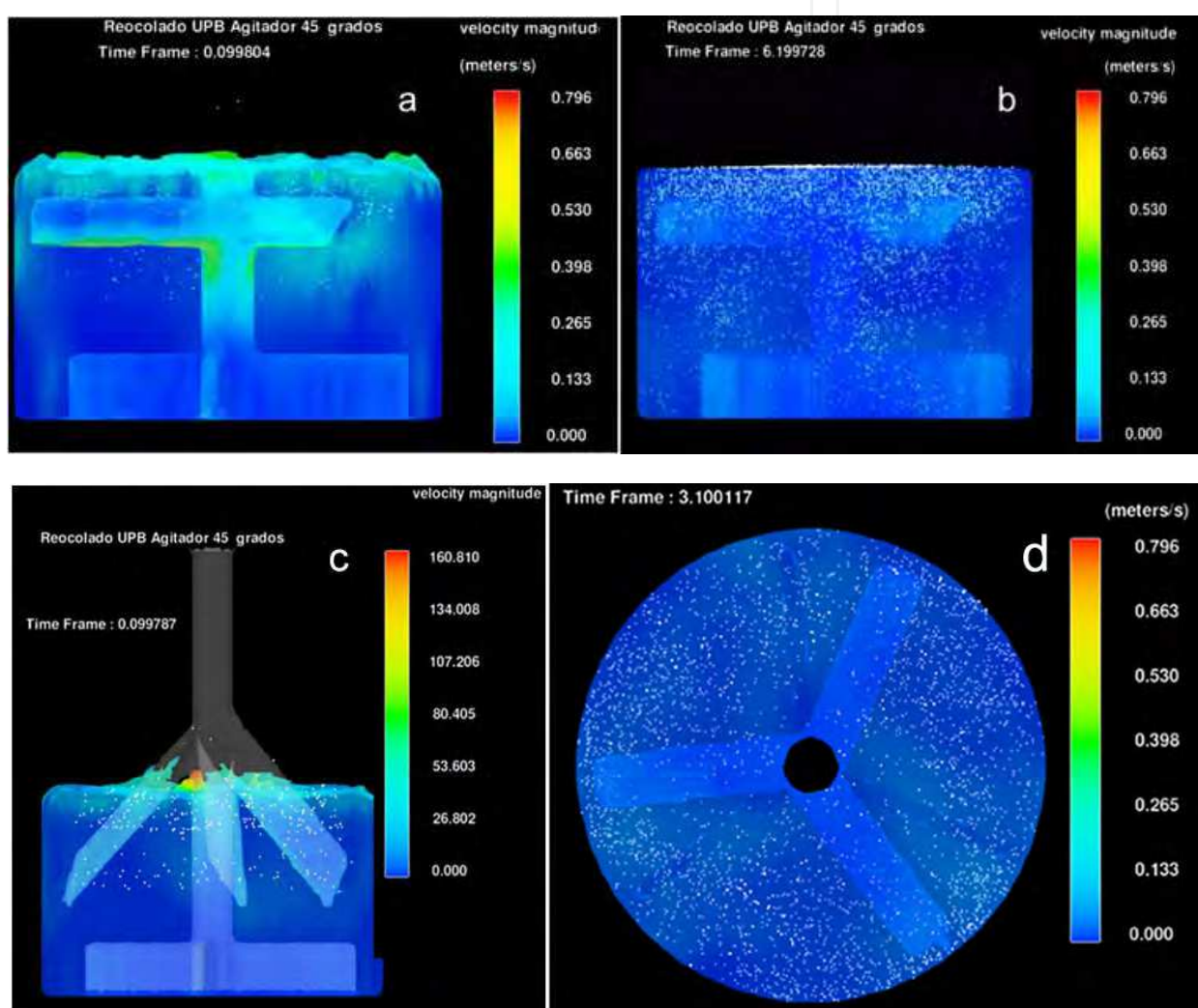


Fig. 8. Simulation of the agitation process. Stirrer speed profile for the 45°-x agitator (a, b), and for the $45^\circ\text{-x}/45^\circ\text{-y}$ agitator (c, d).

3.2.4 Air engulfment

Finally, according to the simulations the condition of air trapping in both mixers is minimal. Neither case produces a pronounced vortex that allows the entry of air into the molten aluminum. At the start of agitation during the first 6s, the trapped air was $\sim 14\text{vol}\%$ (Fig. 9a,

9c). However, after stirring for 20s, the fraction of trapped air drops to $\sim 0.4\text{vol}\%$, indicating that the agitation is effective and does not introduce air into the melt (Fig. 9b, 9d).

For simulations of the MSC process, the $45^\circ\text{-}x/45^\circ\text{-}y$ agitator was selected, since it produced the best results in productivity and process efficiency. Then we proceeded to the synthesis of composite material. In order to control the MSC process in real time (rpm, rotation direction and geometric localization of the stirrer), a LabView® interface was implemented using a National Instruments USB data acquisition (DAQ) device.

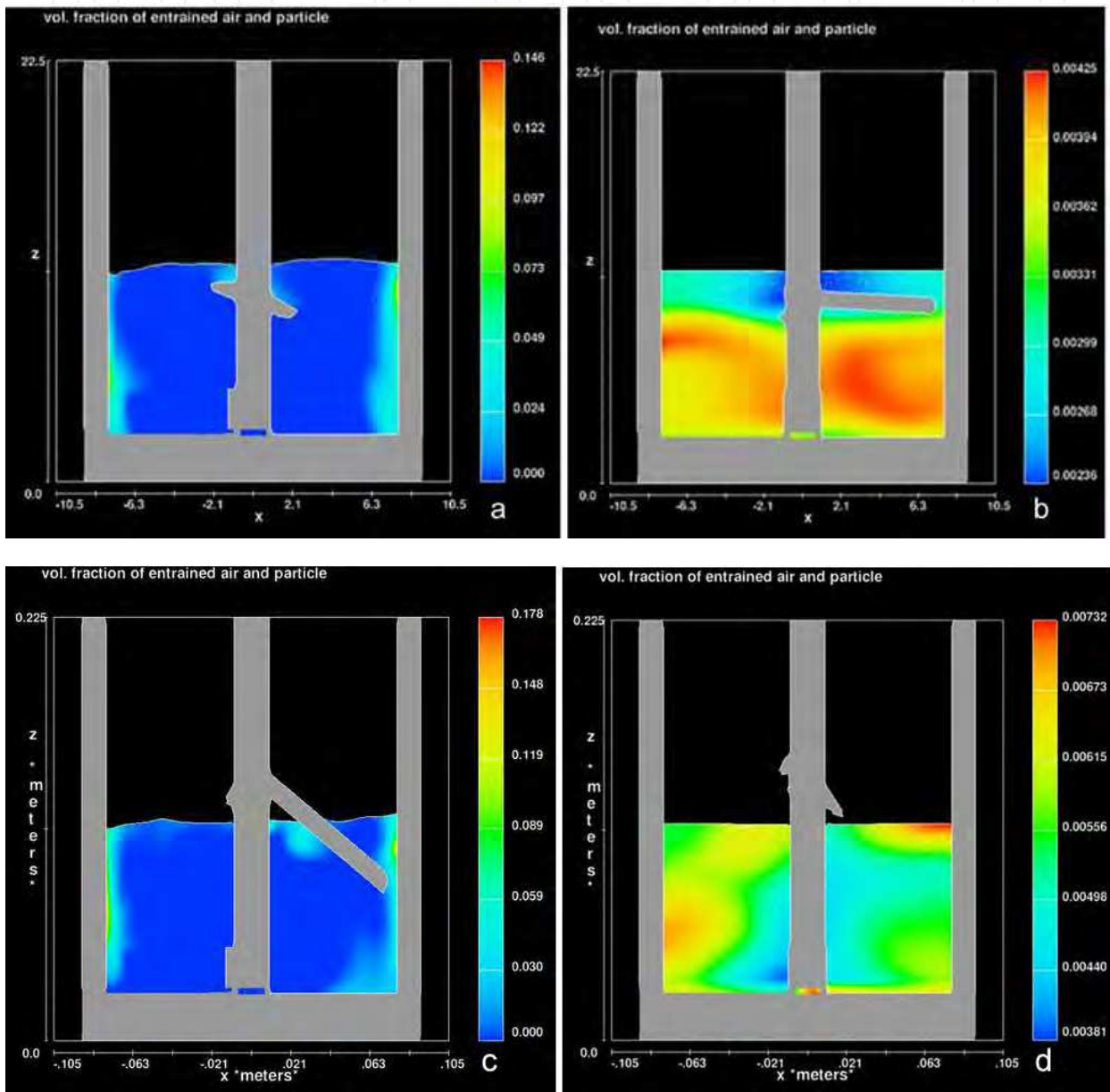


Fig. 9. Simulation of the agitation process. Profile of trapped air stirrer at $45^\circ\text{-}x$ (a, b), agitator $45^\circ\text{-}x/45^\circ\text{-}y$ (c, d). stirring during first 6s (a, c), after 20s (b, d).

Table 4 lists the key parameters used during MSC. The solid fraction is 0.4. Stirring is performed in an argon atmosphere and in an anti-clockwise direction.

Parameters for MSC	Value
Melting temperature (°C)	610
Process temperature (°C)	594
Velocity magnitude (rpm)	600
Stirring conditions (min, °C)	20, 594
Reinforcement fraction (wt%)	15
Reinforcement size (µm)	<38

Table 4. General parameters for MSC.

Fig. 10 illustrates the microstructural evolution of the semisolid processed material. The resulting morphology consists of α globular phases with a diameter of about 70µm, surrounded by eutectic microconstituents.

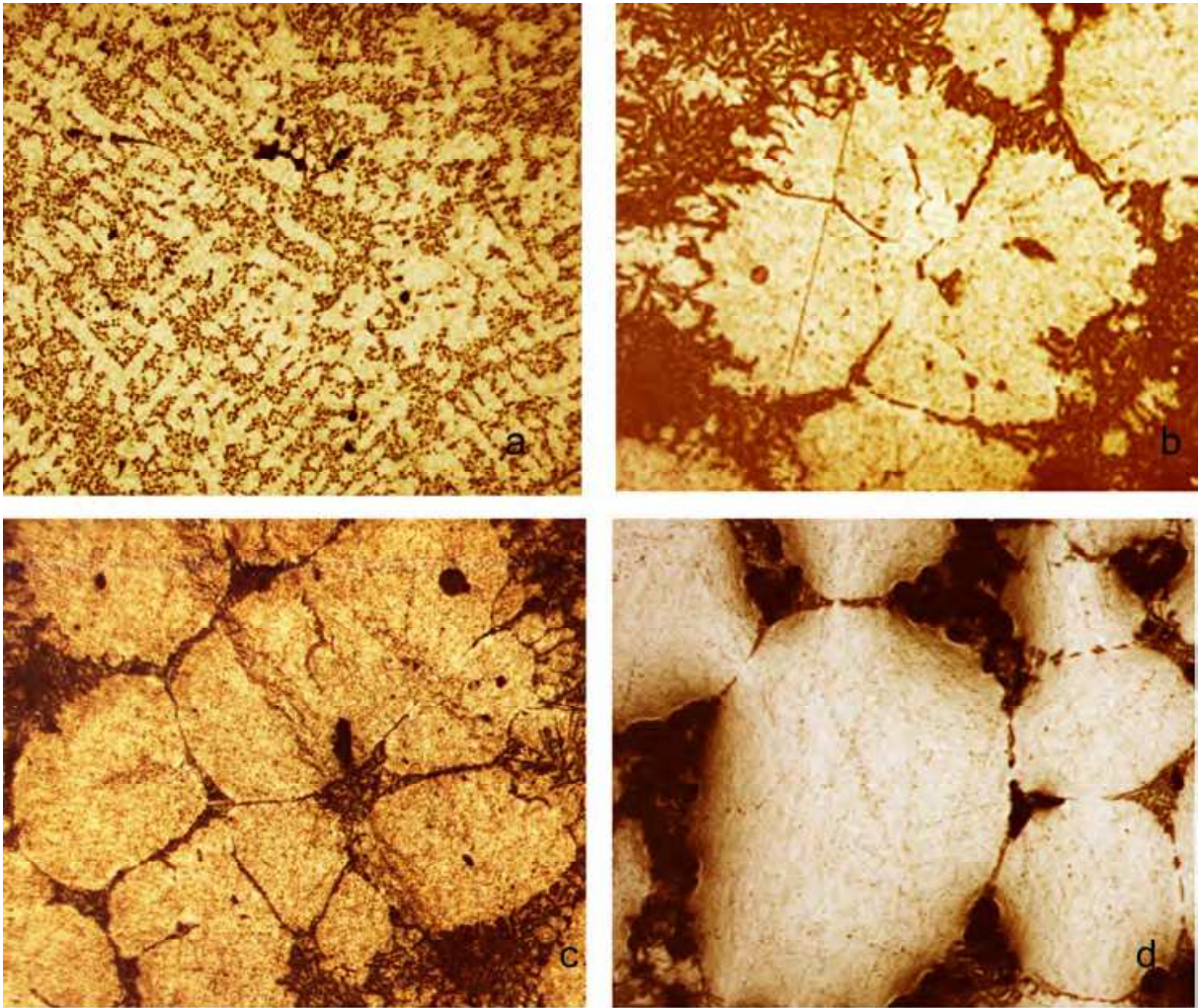


Fig. 10. Optical images of microstructure evolution for the alloy A-356 during the MSC. (a) dendritic structure (50X), (b) rosette type morphology (50X), (c) formation of globular structure (50X), (d) globular structure (including reinforcement particles 50X).

Figs. 11 and 12 shows the morphology obtained after the addition of reinforcement material. Fig. 11a shows the alloy processed by MSC with β -SiC particles. The morphology of the

matrix is completely globular, with grain sizes ranging from 75 to 100 μ m. In Fig. 11b, Fig. 12a and 12c the reinforcement particles are fully dispersed and preferentially located in the eutectic zone. Some faceted forms for the reinforcement particles were observed (Figs. 11b, 12c), which creates fewer opportunities for a mechanical interface with the metal matrix. It can be argued that the interface must be chemical, as it was envisaged during the EP treatment of the reinforced particles, modifying the metal-ceramic interface (SiC-Al) into a metal-metal type interface. At the experimental level there is minor porosity, which must be corrected in the subsequent HPDC process.

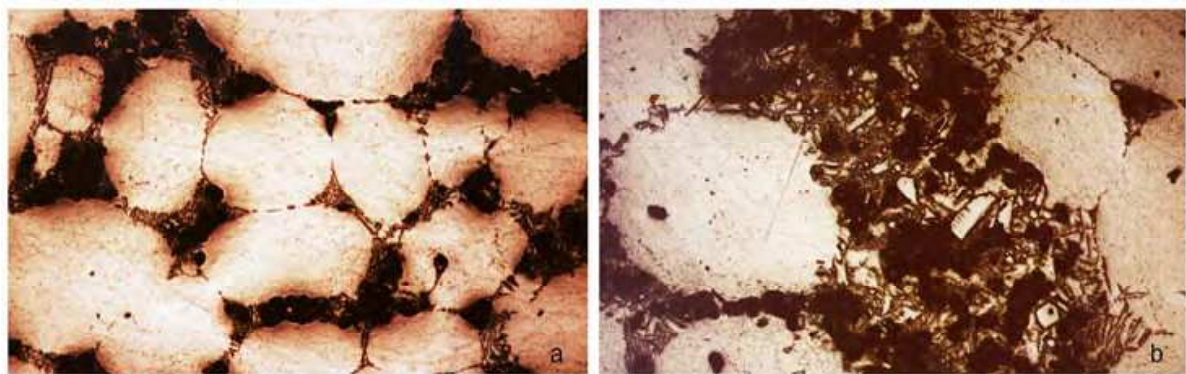


Fig. 11. Optical images of the microstructure of A-356/ β SiC-15wt% composite at (a) 50X and (b) 100X.

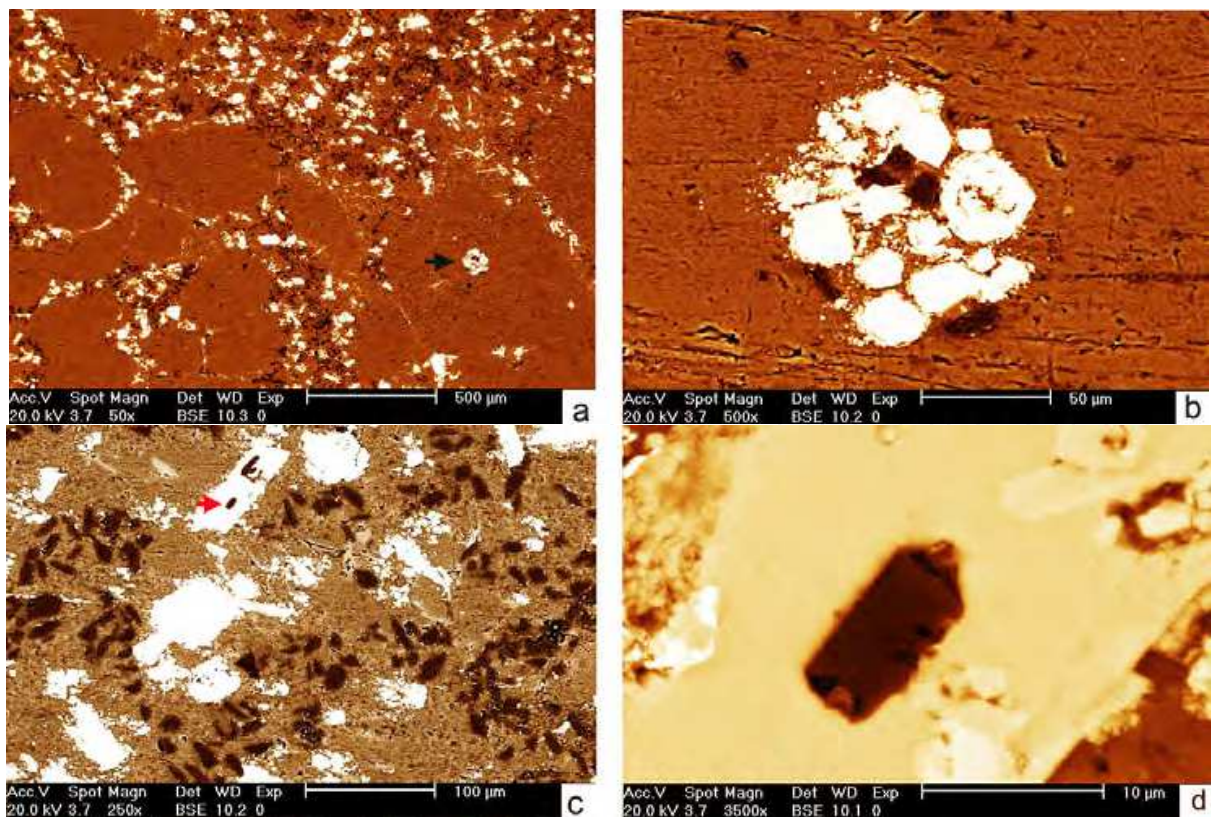


Fig. 12. SEM images of the A-356/ β SiC-15wt% composite; (b) and (d) are magnified views of (a) and (c), respectively, showing reinforcement particles engulfed in eutectic zones.

3.3 High Pressure Die Casting (HPDC)

After obtaining a homogeneous composite, a die cast is made in order to obtain an ingot by applying moderate pressure for 12 to 15s. Our MSC&HPDC (Fig. 13) is useful both for research and production on a laboratory scale. The HPDC has four hydraulic cylinders to provide the load. The HPDC process for an ingot of semisolid material and its solidification take place when a pressure ranging from 50 to 100 MPa is applied. Other parameters are listed in table 5. This device has no striker ejection pin; instead, after the hydraulic cylinders are opened, the part falls to a container located at the bottom of the device.

Parameters for HPDC	Value
Pouring temperature (°C)	594
Mold temperature (°C)	250
Load (MPa)	50-100

Table 5. General parameters for HPDC.

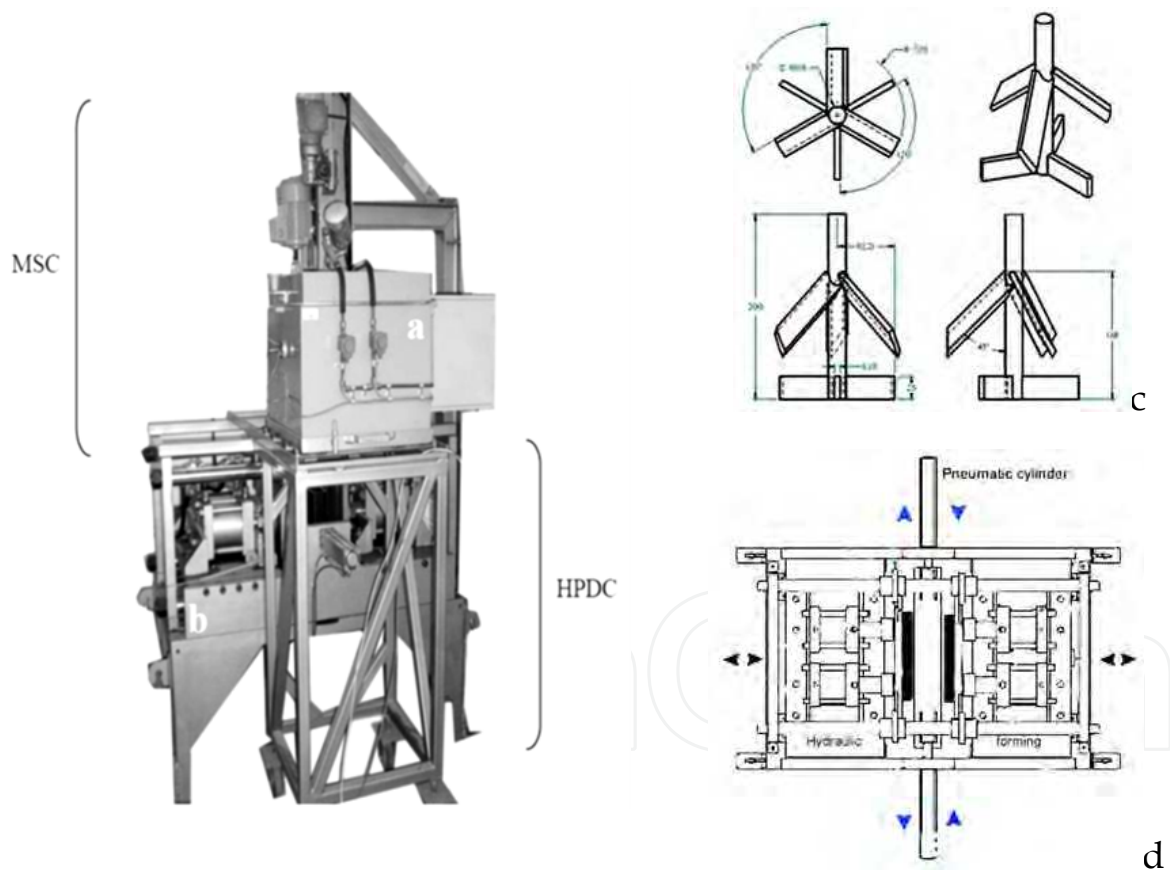


Fig. 13. MSC&HPDC device: (a, c) Mechanical stir casting unit; (b, d) High pressure die casting (shaping) unit.

3.3.1 Computational fluid dynamics simulation

The semisolid forging process of a piece was initially simulated using CFD tools (Flow-3D®). Fig. 14 shows an image of the simulated part. With this simulation it is possible to

determine zones where defects could develop instantly, as well as sites where interlaminar differences could generate irregular and turbulent flow. This figure also shows the velocity profile in three different moments for the piece. It can be seen that in the external part of the mold there is an increase in the velocity of the flow. Despite the high velocity, at each of the time intervals analyzed, the outer or leading surface of the material inside the mold is homogenous, thus avoiding defects by gas inclusion.

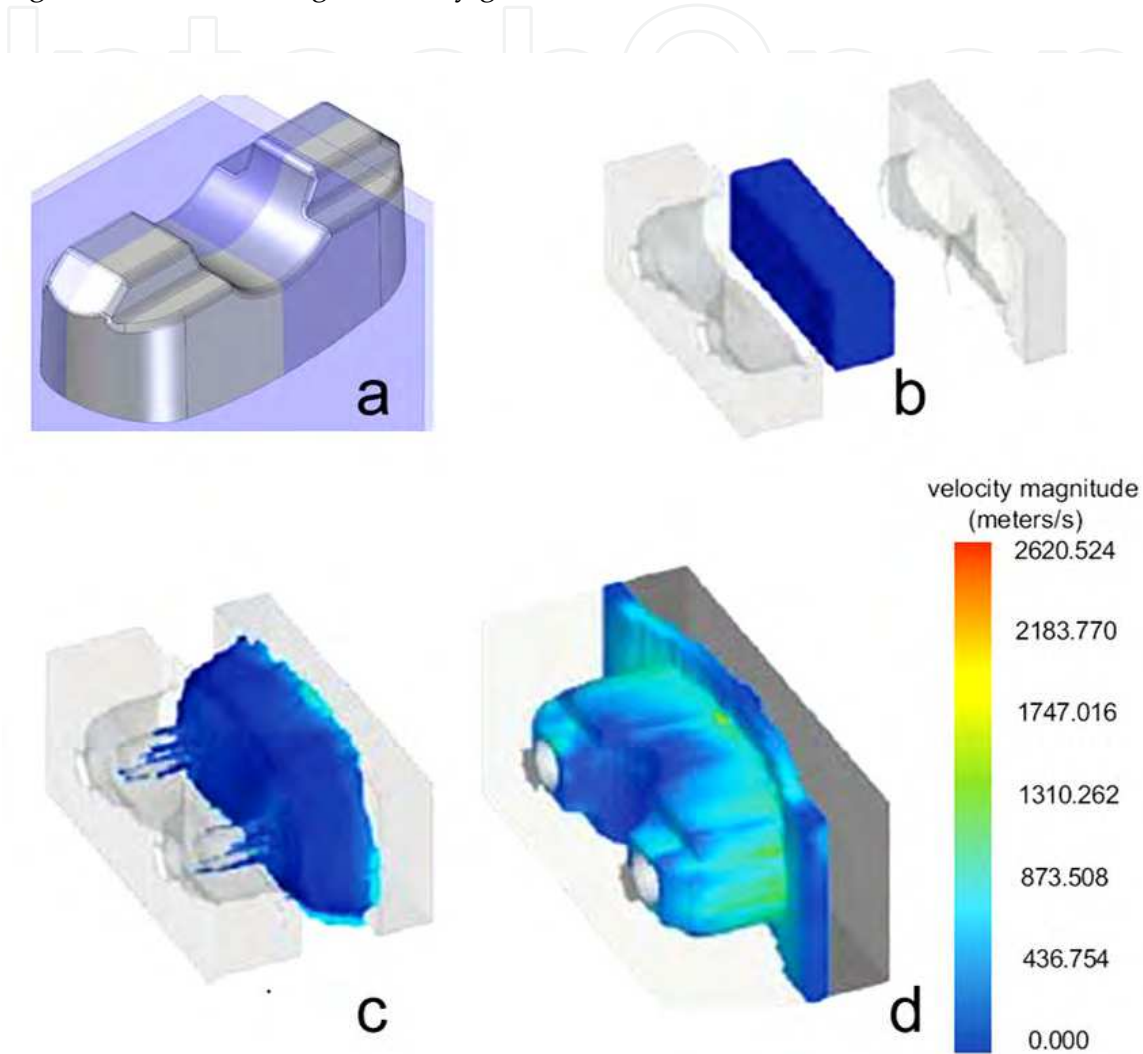


Fig. 14. Computational fluid dynamics analysis of piece to be created by HPDC (a) shape of the final part , (b) initial position of the ingot and mold, (c-d) velocity profiles at two stages of pressing of the composite paste.

3.3.2 Manufacture and heat treatment

After verifying the integrity of the piece through the simulation of the HPDC process, manufacture was carried out using the parameters of pressure and application load times mentioned above. Importantly, prior to the HPDC process the preformed mold and the mold (Fig. 14b) were heated to 300°C. The piece underwent thermal treatment in solution at 548°C for 8h, followed by cooling in water and artificial aging (T6) at 170°C, for 6h and cooled with air. Fig. 15 shows the HPDC piece and molds.



Fig. 15. (a) HPDC molds, and (b) resultant piece produced by MSC&HPDC.

4. Mechanical characterization

The dispersion of stiff ceramic particles or fibers within a ductile metallic matrix leads to an increase in flow stress of the metal by load transfer across a strong interface from the matrix to the reinforcement (Mortensen & Llorca, 2010). Table 6 summarizes the mechanical properties of the materials processed by MSC&HPDC as compared with nominal A-356 T6 alloy with no reinforcement (Fig. 16a). It is evident that an increase in mechanical resistance and a reduction in the elongation percentage were achieved, demonstrated by the high rigidity of the composite compared with the nominal alloy.

Property	Al-Si7-Mg0.3-T6	Al-Si7-Mg0.3-T6/ β -SiC-15wt%
Ultimate strength (MPa)	220	380
Yield strength (MPa)	180	345
Elongation percentage (%)	18	10
Hardness (HB)	110	130

Table 6. Mechanical properties of processed materials

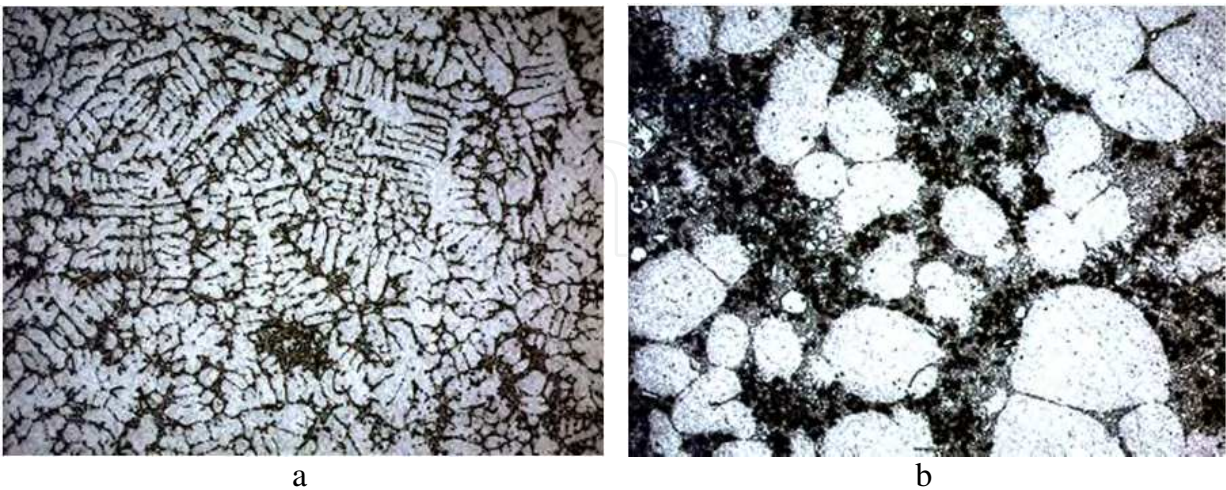


Fig. 16. Comparison of microstructures of materials processed by MSC&HPDC at 50X (a) Al-Si7-Mg0.3-T6 alloy and (b) (Al-Si7-Mg0.3-T6/ β -SiC-15wt%)-T6 composite. Both parts were thermally treated in solution at 548°C for 8h, followed by cooling in water and artificial aging (T6) at 170°C, for 6h and cooled with air.

5. Conclusions

Although research on the subject of MMCs reached a high level of intensity in the late 1980s and early 1990s, interest continues today, albeit in a wider array of more distinct directions, as for example, reported here for the production of pieces from Al-MMC/ β -SiC that can be used in different applications.

Micrometric β -SiC particles, obtained by controlled pyrolysis of rice husk have been modified with Cu through electroless plating (EP). EP coatings enhance the adhesion between Al and β -SiC.

A novel technique for manufacturing parts from MMCs has been designed and tuned. Since the device and processing routes are similar to the conventional ones used in casting, it is safe to say that mechanical stirring coupled with semisolid forging shows interesting advantages, including its low cost, easy process implementation, and the ability to form diverse, near-net-shape parts.

A composite Al-Si7-Mg0.3-T6/ β -SiC-15wt% has been processed by MSC&HPDC and improved mechanical properties were achieved. This process could be useful for producing parts for various industries, including automotive applications.

6. Acknowledgment

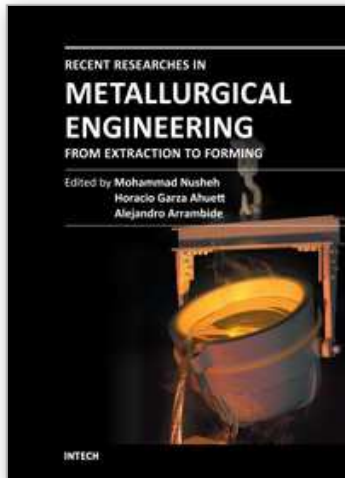
This work has been made possible thanks to the support of COLCIENCIAS, the Engineering School of Antioquia and the Pontificia Bolivariana University in Medellin. Additional thanks to Dr. Mike Boldrick for his valuable suggestions on this document.

7. References

- Biswas, P., Godiwalla, K., Sanyal, D., & Dev, S. (2002). A simple technique for measurement of apparent viscosity of slurries: sand-water system. *Materials and Design*, Vol. 23, No. 5, pp. 511-519. ISSN 0261-3069.
- Fan, Z. (2002). Semisolid metal processing, *International Materials Reviews*, Vol. 47, No. 2, (April 2002), pp. 49-85, ISSN 0950-6608.
- Ghomashchi, M. R. & Vikhrov, A. (2000). Squeeze casting: an overview. *Journal of Materials Processing Technology*. Vol. 101, (April 2000), pp. 1-9. ISSN 0924-0136.
- Kim, I. S. and Lee, S. K. (2005). Fabrication of carbon nanofiber/Cu composite powder by electroless plating and microstructural evolution during thermal exposure. *Scripta Materialia*, Vol. 52, No. 10, (May 2005), pp. 1045-1049. ISSN 1359-6462.
- Mada, M., & Ajersch, F. (1996). Rheological model of semisolid A356-SiC composite alloys. Part I: Dissociation of agglomerate structures during shear. *Materials Science and Engineering A*, Vol. 212, No. 1, (July 1996), pp. 157-170. ISSN 0921-5093.
- Martinez, H. V.; Valencia M. F.; Chejne, F. & Cruz, L. (2006). Production of β -SiC by pyrolysis of rice husk in gas furnaces. *Ceramics International*, Vol. 32, (December 2006), pp.891-897, ISSN 0272-8842.
- Martinez, V.; Valencia, M. Compocasting process of cast Zamak particulate composites. *Frontiers in Materials Research, A CIAM-CIMAT-CONICYT WORKSHOP*, p. 68, Viña del Mar, Chile, 26-29 April 2004.

- Mortensen, A., & Llorca, J. (2010). Metal Matrix Composites. *Annual Review of Materials Research*, Vol. 40, No. 1, pp. 243-270.
- Sharmaa, R., Agarwala, R.C. & Agarwala V. (2006). Development of copper coatings on ceramic powder by electroless technique. *Applied Surface Science*. Vol. 252, No. 24, (October 2006), p.p. 8487-8493. ISSN 0169-4332.
- V. Laurent, C. Rado & N. Eustathopoulos (1996). Wetting kinetics and bonding of Al and Al alloys on α -SiC. *Materials Science and Engineering A*. Vol. 205, (January 1996), pp 1-8, ISSN 0921-5093.
- Yang, Z. Kang, C.G. & Seo, P.K. (2005). Evolution of the rheocasting structure of A356 alloy investigated by large-scale crystal orientation observation, *Scripta Materialia*, Vol. 52, No. 4, (February 2005), pp. 283–288, ISSN 1359-6462.

IntechOpen



Recent Researches in Metallurgical Engineering - From Extraction to Forming

Edited by Dr Mohammad Nusheh

ISBN 978-953-51-0356-1

Hard cover, 186 pages

Publisher InTech

Published online 23, March, 2012

Published in print edition March, 2012

Metallurgical Engineering is the science and technology of producing, processing and giving proper shape to metals and alloys and other Engineering Materials having desired properties through economically viable process. Metallurgical Engineering has played a crucial role in the development of human civilization beginning with bronze-age some 3000 years ago when tools and weapons were mostly produced from the metals and alloys. This science has matured over millennia and still plays crucial role by supplying materials having suitable properties. As the title, "Recent Researches in Metallurgical Engineering, From Extraction to Forming" implies, this text blends new theories with practices covering a broad field that deals with all sorts of metal-related areas including mineral processing, extractive metallurgy, heat treatment and casting.

How to reference

In order to correctly reference this scholarly work, feel free to copy and paste the following:

H. Vladimir Martínez and Marco F. Valencia (2012). Semisolid Processing of Al/ β -SiC Composites by Mechanical Stirring Casting and High Pressure Die Casting, Recent Researches in Metallurgical Engineering - From Extraction to Forming, Dr Mohammad Nusheh (Ed.), ISBN: 978-953-51-0356-1, InTech, Available from: <http://www.intechopen.com/books/recent-researches-in-metallurgical-engineering-from-extraction-to-forming/semisolid-processing-of-al-sic-composites-by-mechanical-stirring-casting-high-pressure-die-casting>

INTECH
open science | open minds

InTech Europe

University Campus STeP Ri
Slavka Krautzeka 83/A
51000 Rijeka, Croatia
Phone: +385 (51) 770 447
Fax: +385 (51) 686 166
www.intechopen.com

InTech China

Unit 405, Office Block, Hotel Equatorial Shanghai
No.65, Yan An Road (West), Shanghai, 200040, China
中国上海市延安西路65号上海国际贵都大饭店办公楼405单元
Phone: +86-21-62489820
Fax: +86-21-62489821

© 2012 The Author(s). Licensee IntechOpen. This is an open access article distributed under the terms of the [Creative Commons Attribution 3.0 License](https://creativecommons.org/licenses/by/3.0/), which permits unrestricted use, distribution, and reproduction in any medium, provided the original work is properly cited.

IntechOpen

IntechOpen